Surface Magnetism: Photoemission Electron Microscopy

1. Introduction

A Photoemission Electron Microscope (PEEM) images photo and/or secondary electrons, which are generated at the surface of a solid sample by the absorption of x-ray or ultraviolet (UV) radiation. Depending on the wavelength of the radiation different contrast mechanisms are present, providing information on the elemental and chemical composition, and the electronic and magnetic properties of the material. Magnetic domain imaging is a major application of the PEEM technique, exploiting the large x-ray magnetic dichroism effect at the L edges of the magnetic 3d transition metals (e.g. Cr, Mn, Fe, Co, Ni) and the M edges of rare earth ferromagnets (e.g. Gd). Here, the PEEM technique will be described and applications in thin film magnetism research will be discussed. For a comparison with other domain imaging techniques see **Kerr Microscopy**, **Magnetic Materials: Transmission Electron Microscopy**, **Magnetic Force Microscopy**, and **Bitter Techniques** and references therein.

The PEEM technique stands out against other magnetic imaging techniques through its surface sensitivity and element specificity, making PEEM an ideal tool for the investigation of ultra-thin magnetic films, multi-layers, and alloys. In contrast to other high resolution, magnetic imaging techniques PEEM is also sensitive to antiferromagnetic order. The spatial resolution of PEEM for magnetic domain imaging is typically about 50-100 nm, which positions PEEM between **Transmission Electron Microscopy** and on the other side optical techniques, such as **Kerr Microscopy.**

2. Photoemission Electron Microscopy

PEEM was first used in the 1930's and has since then matured into an established surface science technique (Stöhr et al 1993, Tonner et al. 1995, Stöhr et al. 1998). PEEM is closely related to the Low Energy Electron Microscope (LEEM) and the Spin-Polarized Low Energy Electron Microscope (SPLEEM), which were pioneered by (Bauer et al. 1994, Duden et al. 1998). PEEM and LEEM both utilize low energy electrons to form an image representing physical properties of the sample surface. LEEM and SPLEEM image diffracted low energy electrons and thereby provide information on the local crystallographic (LEEM) and magnetic (SPLEEM) structure of the surface of a crystalline sample. PEEM in contrast utilizes electrons generated by photo ionization and therefore is not limited to the study of crystalline samples (see also **Photoemission: Spin-polarized and Angle-resolved**). As light sources UV gas discharge lamps, UV lasers and synchrotron radiation sources have been used. Synchrotron radiation offers the important advantage of tunability of the wavelength of the illumination, thereby allowing a selection between various mechanisms of contrast. X-ray PEEM thus combines aspects of spectroscopic and microscopic methods and is called a spectromicroscopy technique.

A typical PEEM setup using synchrotron radiation from a bending magnet is shown in Fig. 1 (Anders et al 1999, Scholl et al 2002). X-rays pass through a moveable aperture, which selects the polarization of the radiation, and are dispersed by an x-ray grating, operating in grazing incidence. An exit slit selects monochromatic radiation, which then illuminates the sample in the focus of the microscope column. Polarization control is essential in magnetic imaging, giving access to the magnetic dichroism effects. A schematic kinetic energy spectrum of the emitted electrons after absorption of x-rays is shown in Fig. 2a. Photoemission lines appear at high kinetic energy, followed by a wide tail of secondary electrons which peak at low energies close to the work function cut-off. PEEM microscopes usually accept the total electron yield without

energy analysis. The sampling depth of PEEM depends on the mean free path of low energy electrons in the studied material and lies typically between 2 and 5 nm for metals. The emitted electrons are accelerated in the strong electric field between the sample and the first microscope lens (~10^4V/mm), and are then imaged with magnification by an electron optics, consisting of typically 2-4 electrostatic or magnetic lenses. A back focal plane aperture limits the angular spread of the transmitted electrons and also acts as a simple energy filter, reducing the chromatic and spherical aberrations of the microscope. One or two projector lenses magnify and focus the image onto the electron detector, typically an electron sensitive phosphor or/and a channelplate detector, which produces a visible image. Deflector and stigmator elements in the microscope steer the electron beam and correct for eventual mechanical misalignments. Using synchrotron radiation microscopes have achieved a spatial resolution close to 20 nm (Anders et al 1999).

3. Contrast mechanisms:

Contrast in PEEM results from local variations in the light absorption cross-section, the work function and the topography of the sample. Topographic structures such as edges, bumps and holes locally distort the electric field close to the sample and modulate the image intensity. Work function contrast arises from inhomogeneities in the surface composition and thereby work function and is particularly strong using ultraviolet excitation close to the work function cut-off.

Chemical, magnetic and elemental contrast arises from the Near Edge X-ray Absorption Fine Structure (NEXAFS), which is discussed in detail in **Surface Chemistry: Electron Yield Spectroscopy**. As an example, an x-ray absorption spectrum of a Co/FeMn/NiO multi-layer is shown in Fig. 2b. Different elements can be identified by their characteristic absorption resonances. The fine structure close to the absorption edge – the inset shows the Ni $L_{2,3}$ edge – can be further analyzed, providing information about the chemical and magnetic state of the material. The multiplet structure at the L edges, marked by arrows, is characteristic for nickel

oxide (Regan et al 2001). PEEM microscopes are typically used in three modes of operation: a) full-field imaging, b) local spectroscopy, and c) spectromicroscopy. In the full-field imaging mode images are acquired at fixed photon energy. In the local spectroscopy mode local x-ray absorption spectra are acquired in predefined regions by scanning the photon energy and using the spatial resolution provided by the PEEM electron optics. In the spectromicroscopy mode, stacks of PEEM images are acquired as function of photon energy, generating a three dimensional dataset with two lateral and one energy dimension. Stacks are post-analyzed and provide complete information on the chemical, electronic and magnetic properties of the sample surface, pixel-by-pixel.

3. X-ray Magnetic Linear and Circular Dichroism

X-ray Magnetic Circular Dichroism (XMCD) and X-ray Magnetic Linear Dichroism (XMLD) are established spectroscopic x-ray techniques, which are widely used for the investigation of ferromagnetic and antiferromagnetic surfaces and thin films (Thole et al. 1985, Schütz et al. 1987, Alders et al. 1998, see also **Magnetism: Applications of Synchrotron Radiation**). Both methods probe the modification of the electronic structure of a material in the presence of magnetic order, resulting in an intensity variation of the near edge x-ray absorption fine structure. X-ray magnetic dichroism has been extensively used at the dipole allowed, 2p to 3d transitions ($L_{2,3}$ edge) exploiting the strong spin-orbit interaction at the 2p core levels and the strong exchange splitting of the 3d valence levels (Schütz et al. 1987). More recently XMLD has been applied in studies of collinear antiferromagnets (e.g. Alders et al. 1998). In order to illustrate these dichroism effects x-ray absorption spectra are shown in Fig. 3, measured in single microscopic magnetics domains on a) a ferromagnetic Co film and b) an antiferromagnetic $LaFeO_3$ film using PEEM. The relative orientation of the photon polarization and the sample magnetization are shown on the right. The size of the XMCD effect in Co, which appears as a

variation of the L_3 and L_2 resonance intensities depending on the relative orientation of the sample magnetization **M** and the circular x-ray polarization direction **P**, is a measure for the element specific, atomic, spin and orbital moment and also the angle enclosed by the magnetization and the polarization vector: $\Delta I \sim |\mathbf{M}| \cos \angle(\mathbf{M}, \mathbf{P})$. In contrast, XMLD is particularly useful for the investigation of antiferromagnets since these do not possess a macroscopic magnetization that can be detected using XMCD. The near edge fine structure in the absorption of linearly polarized x rays is sensitive to an anisotropic electronic structure, e.g. resulting from a collinear magnetic order of the sample. For example, the absorption spectrum of Fe in the antiferromagnet $LaFeO_3$ shows a change in the relative intensity of the multiplet peaks at the L_3 and L_2 edges, depending on the relative orientation of the $LaFeO_3$ magnetic axis and the linear x-ray polarization. The size of the effect is again a measure for the element specific, atomic, magnetic moment **M** and the angle enclosed by the spin axis **A** and the linear polarization vector **E**: $\Delta I \sim |\mathbf{M}^2| \left(1 - 2\cos^2 \angle(\mathbf{A}, \mathbf{E})\right)$.

XMCD has been first applied to ferromagnetic domain imaging in a pioneering work in 1993 by (Stöhr et al 1993). More recently microscopic antiferromagnetic domains have been imaged for the first time using XMLD (Scholl et al 2000, Nolting et al 2000). For the study of ferromagnetic domains in transition metal ferromagnets, e.g. Co, images are acquired with the photon energy tuned to the peak of the L_3 and L_2 resonances (Fig. 3a). Since the XMCD effect shows an opposite sign at the two L resonances, the magnetic contribution to images can be enhanced and non-magnetic effects can be suppressed by dividing the L_3 and L_2 images (Fig. 4a). The ratio image acquired with circular polarization is called XMCD image. Similarly, dividing PEEM images acquired at the magnetically sensitive peaks A and B at the L_2 edge of the antiferromagnet $LaFeO_3$ (Fig. 3b) yields the XMLD image, repesenting the antiferromagnetic

domain structure of the material (Fig. 4b). Different colors in the XMCD and XMLD image correspond to different directions of the magnetic moment as explained in the color legend. In Co (top) we distinguish three classes of domains, which have magnetizations pointing up (blue), down (yellow), and left or right (green, not distinguished in this geometry). The XMLD image of $LaFeO_3$ shows two classes of domains with the in-plane projection of the atomic magnetic moments pointing up-down (dark blue) and left-right (light blue). The studied sample is a $Co/LaFeO_3$ bi-layer, grown on $SrTiO_3(001)$ (REF) with a Co thickness of about 1.2nm and a $LaFeO_3$ thickness of 40 nm. Note, that the shown images were acquired at identical sample positions, making use of the element specificity of x-ray PEEM. The correspondence between the two domain structures indicates a uniaxial interface exchange coupling of sufficient strength, aligning the magnetization in the ferromagnet with the in-plane component of the magnetic axis in the antiferromagnet. Due to its relatively moderate surface sensitivity and the elemental specificity, x-ray PEEM is particularly useful for the study of such magnetic coupling phenomena in layered ultrathin films.

4. Imaging of local exchange bias

One important application of domain imaging using the PEEM technique is the study of exchange biased thin film systems. Exchange bias at a ferromagnet/antiferromagnet interface leads to a unidirectional anisotropy of the ferromagnetic layer, pinning its magnetization into a preferred direction, which is set by cooling the structure in an external magnetic field down through the magnetic ordering temperature of the antiferromagnet (Néel temperature) (Meiklejohn et al. 1956), see also **Magnetic Films: Anisotropy**. This pinning is employed in magneto-electronic devices for stabilization of the magnetization in a magnetic reference layer. The major application of this effect is in magnetic hard disk heads containing a read element based on the **giant magnetoresistance** phenomenon (see also **Magnetic Recording**

Technologies: Overview). The unique combination of elemental specificity, surface sensitivity, and ferro- and antiferromagnetic contrast of PEEM allows studying the magnetic structure directly at the interface between two coupled layers, providing crucial insight into the microscopic coupling mechanism (Ohldag et al. 2001). Exchange bias in a ferromagnet/antiferromagnet bi-layer leads to a pinning of the magnetization domain-by-domain and an asymmetry of the magnetization reversal process as shown in Fig. 5. XMCD images of a ferromagnetic Co layer in contact with the antiferromagnet $LaFeO_3$ were acquired in remanence as function of the applied magnetic field. Fig. 5 shows a subset of a complete field series, which contains about 30 images per field cycle. Cycling was repeated several times in order to check the reproducibility of the measurement. After application of a strong negative field aligned with the in-plane projection of the photon polarization, increasing positive field pulses were applied and XMCD images were acquired as function of field strength. The strong uniaxial interface coupling to the AFM prevents a permanent rotation of the horizontally oriented magnetic domains (gray), which have a magnetization oriented perpendicular to the field direction. Vertically oriented domains, which have an easy axis along the magnetic field, change from black to white at about 100 Oe, indicating the switching of the magnetization direction parallel to the applied field. Remanent hysteresis loops of two individual domains are shown at the bottom of Fig. 5. The two representative loops show a relative shift of the plus/minus and minus/plus switching fields of about 50 Oe. This corresponds to a positive (negative) exchange bias field in the green (magenta) domain of +25 (-25) Oe. Repeating this analysis pixel-by-pixel generates maps of the local bias field, providing information on the dependence of the pinning strength with the structure of the antiferromagnet, e.g. the antiferromagnetic domain size. Averaging over a large number of domains yields the average loop (black), which shows half the amplitude compared with loops of individual domain because the applied field switches only 50% of the domains.

5. Conclusion

In comparison to other domain imaging techniques x-ray PEEM stands out by its ability to separately study the chemical, electronic and magnetic properties of different materials in a layered or alloyed material. The moderate surface sensitivity of the technique permits the investigation of ultrathin multilayers but at the same time is sufficiently sensitive to detect sub-monolayer amounts of magnetic moments. The spatial resolution of magnetic PEEM can be improved by the introduction of aberration correction schemes. By correction of the aberrations of the electron optical system PEEM should reach a spatial resolution of below 5 nm, close to the physical limit given by the mean free path of electrons in matter (2 nm in metals). Aberration corrected microscopes will be especially useful for the investigation of disordered, granular materials, which are used in technologically important magnetic devices. The typical grain diameter in granular magnetic structures is typically about 5-20 nm. Another potential application of PEEM is the investigation of dynamical magnetic processes such as spin precession and magnetization reversal utilizing the pulsed structure of synchrotron sources

Bibliography

J. Stöhr, Y. Wu, B.D. Hermsmeier, M.G. Samant, G.R. Harp, S. Koranda, D. Dunham, and B.P. Tonner, Element specific magnetic microscopy with circularly polarized x-rays, Science **259** (1993) 658-661

B.P. Tonner, D. Dunham, T. Droubay, J. Kikuma, J. Denlinger, E. Rotenberg, and A. Warwick, The development of electron spectromicroscopy, J. Electron Spectrosc. Rel. Phenom. **75** (1995) 309-332

J. Stöhr, H.A. Padmore, S. Anders, T. Stammler, and M.R. Scheinfein, Principles of x-ray magnetic dichroism spectromicroscopy, Surf. Rev. Lett. **5** (1998) 1297-1308

E. Bauer, Low energy electron microscopy, Rep. Prog. Phys. **57** (1994) 895-938

T. Duden and E. Bauer, Spin-polarized low energy electron microscopy, Sur. Rev. Lett. **5** (1998) 1213-1219

S. Anders, H. A. Padmore, R. M. Duarte, T. Renner, Th. Stammler, A. Scholl, M. R. Scheinfein, J. Stöhr, L. Séve, and B. Sinkovic, Photoemission Electron Microscope for the study of magnetic materials, Rev. Sci. Instrum. **70** (1999) 3973-3981

A. Scholl, H. Ohldag, F. Nolting, J. Stöhr, H.A. Padmore, X-ray photoemission electron microscopy, a tool for the investigation of complex magnetic structures, Rev. Sci. Instrum. **73** (2002) 1362-1368

D. Alders, L.H. Tjeng, F.C. Voogt, T. Hibma, G.A. Sawatzky, C.T. Chen, J. Vogel, M. Sacchi, and S. Iacobucci, Temperature and thickness dependence of magnetic moments in NiO epitaxial films, Phys. Rev. B **57** (1998) 11623-11631

T. J. Regan, H. Ohldag, C. Stamm, F. Nolting, J. Lüning,, J. Stöhr, and R. L. White, Chemical effects at metal/oxide interfaces studied by x-ray-absorption spectroscopy, Phys. Rev. B **64** (2001) 214422/1-11

B.T. Thole, G. van der Laan, and G.A. Sawatzky, Strong magnetic dichroism predicted in the $M_{4,5}$ x-ray absorption spectra of magnetic rare-earth materials, Phys. Rev. Lett. **55** (1985) 2086-2088

G. Schütz, W. Wagner, W. Wilhelm, P. Kienle, R. Zeller, R. Frahm, and G. Materlik, Absorption of circularly polarized x rays in iron, Phys. Rev. Lett. **58** (1987) 737-740

A. Scholl, J. Stöhr, J. Lüning, J.W. Seo, J. Fompeyrine, H. Siegwart, J.-P. Locquet, F. Nolting, S. Anders, E.E Fullerton, M.R. Scheinfein, and H.A. Padmore, Observation of antiferromagnetic domains in epitaxial thin films, Science **287** (2000) 1014-1016

F. Nolting, A. Scholl, J. Stöhr, J.W. Seo, J. Fompeyrine, H. Siegwart, J.-P. Locquet, S. Anders, J. Lüning, E.E. Fullerton, M.F. Toney, M.R. Scheinfein, and H.A. Padmore, Direct observation of the alignment of ferromagnetic spins by antiferromagnetic spins, Nature **405** (2000) 767-769

W.H. Meiklejohn and C.P. Bean, New magnetic anisotropy, Phys. Rev **102**, (1956) 1413-1414

H. Ohldag, T. J. Regan, J. Stöhr, A. Scholl, F. Nolting, J. Lüning, C. Stamm, S. Anders, and R. L. White, Spectroscopic identification and direct imaging of interfacial magnetic spins, Phys. Rev Lett. **87** (2001) 247201/1-4

Figures

Figure 1: PEEM-2 Photoemission Electron Microscope and soft x-ray beamline at the Advanced Light Source (ALS). The x-ray beam is monochromatized using a spherical grating and focused into a 30x30 μm^2 spot on the sample. The electron microscope column uses electrostatic lenses and produces a magnified image of the local x-ray absorption on a phosphor, which is imaged by a slow-scan CCD camera. A back focal plane aperture acts as an energy and angle filter improving the spatial resolution of the microscope.

Figure 2: a) Energy spectrum of emitted electrons after the absorption of x rays. b) X-ray absorption spectrum measured in total electron yield of a Co/FeMn/NiO sample. The absoption fine structure at the Ni L_2 peak (inset) results from the presence of nickel oxide.

Figure 3: a) X-ray Magnetic Circular Dichroism (XMCD) and b) Linear Dichroism (XMLD) spectra of 1.2 nm Co / 40 nm $LaFeO_3$ / $SrTiO_3$(001). The magnetic dichroism spectrum of the $LaFeO_3$ layer was acquired at the Fe edge. Local PEEM spectra, which were acquired in single ferromagnetic (Co) and antiferromagnetic ($LaFeO_3$) domains, show the effect of magnetic dichroism at the L_3 and L_2 resonances. Magnetic domain images are obtained by selecting an x-ray energy at which the absorption is sensitive to the orientation of the magnetic moment (marked by black arrows). The spectrum shows an opposite effect (a) at the L_3 and L_2 resonance in the ferromagnet Co and (b) at the L_2 multiplet peaks A and B in the antiferromagnet $LaFeO_3$.

Figure 4: X-ray magnetic dichroism images of a) the ferromagnetic domain structure in Co and b) the antiferromagnertic domain structure in $LaFeO_3$ in a $Co/LaFeO_3/SrTiO_3(001)$ multilayer sample. Different colors refer to different domain orientations as explained in the color legend. The images were obtained by dividing two PEEM images acquired at the L_3 and L_2 resonance in case of Co, and by dividing two images acquired at peak A and B of the L_2 resonance in case of $LaFeO_3$. This procedure enhances the magnetic and suppresses topographic contrast. The images demonstrate a parallel orientation of the in-plane component of the Fe and Co moment due to interfacial exchange coupling.

Figure 5: a) Magnetization reversal of Co layer pinned by $LaFeO_3$ underlayer. The images were acquired in remance after applying magnetic fields of increasing strength. The correspondence of magnetization direction to domain brightness is illustrated on the right. b) Local hysteresis loops were calculated in single domains, showing exchange bias of opposite sign (green/magenta). The average loop (black) was acquired by averaging the XMCD intensity over the whole PEEM field of view.

Figure 1

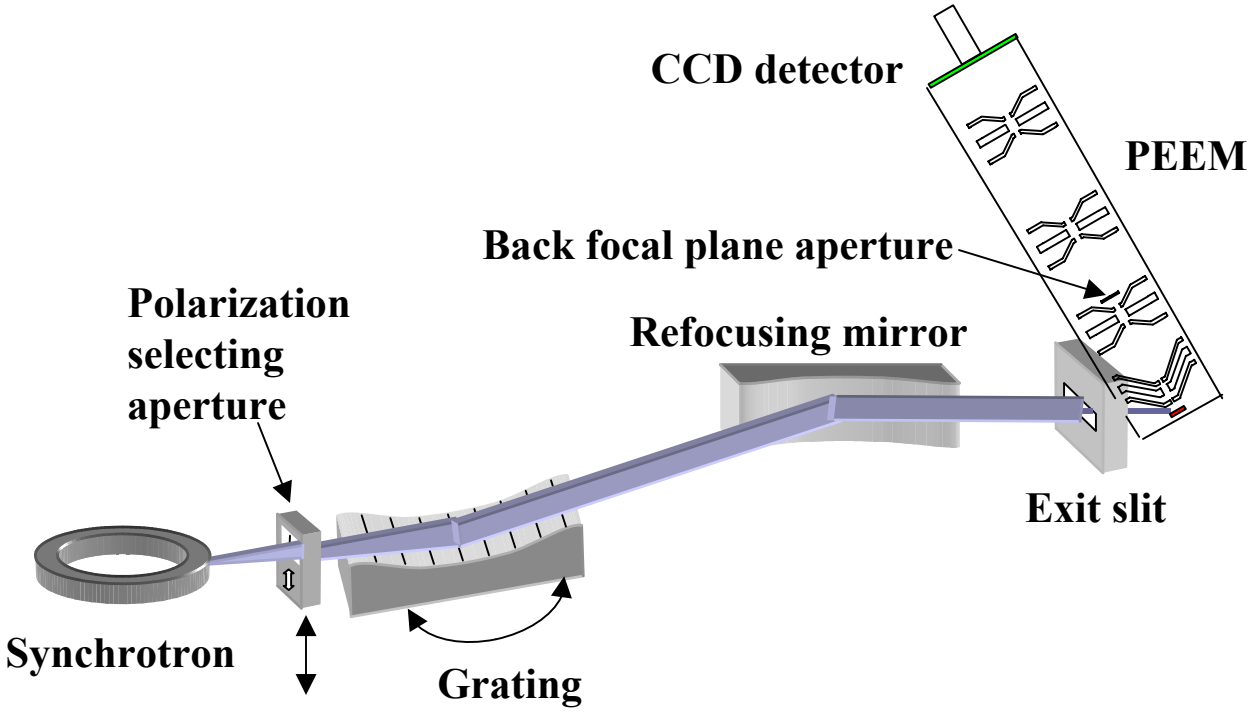
CCD detector
PEEM
Back focal plane aperture
Polarization selecting aperture
Refocusing mirror
Exit slit
Synchrotron
Grating

Figure 2

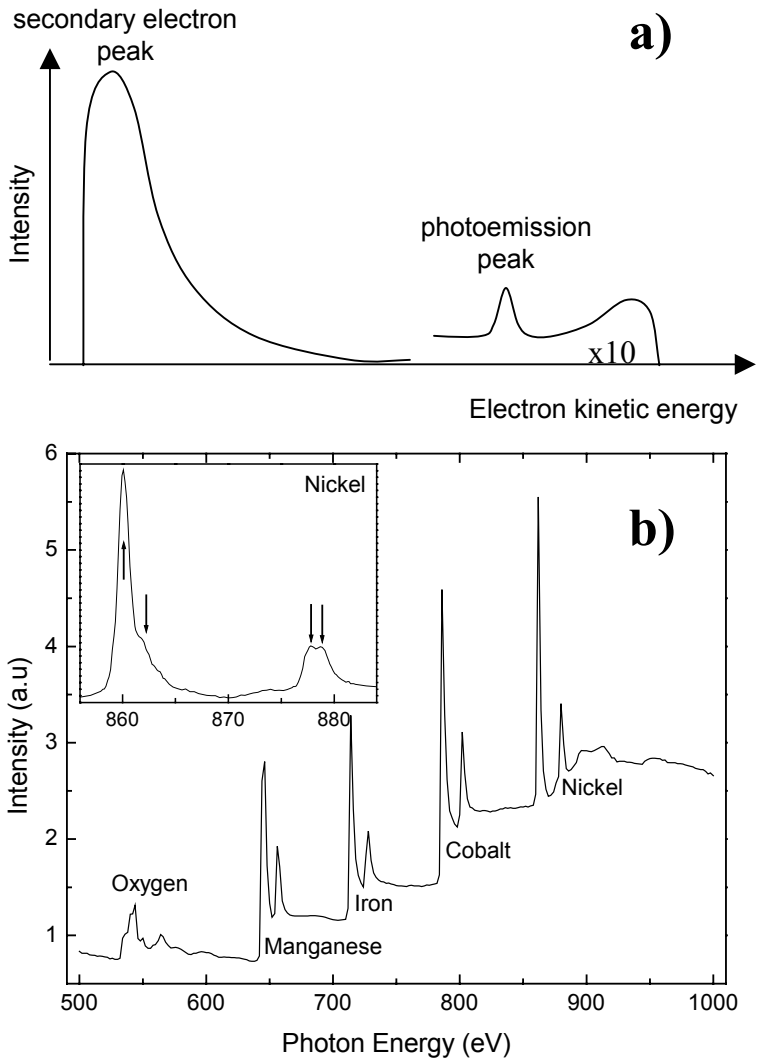
a)
secondary electron peak
Intensity
photoemission peak
x10
Electron kinetic energy
b)
Nickel
860
870
880
Intensity (a.u)
Oxygen
Manganese
Iron
Cobalt
Nickel
500
600
700
800
900
1000
Photon Energy (eV)

Figure 3

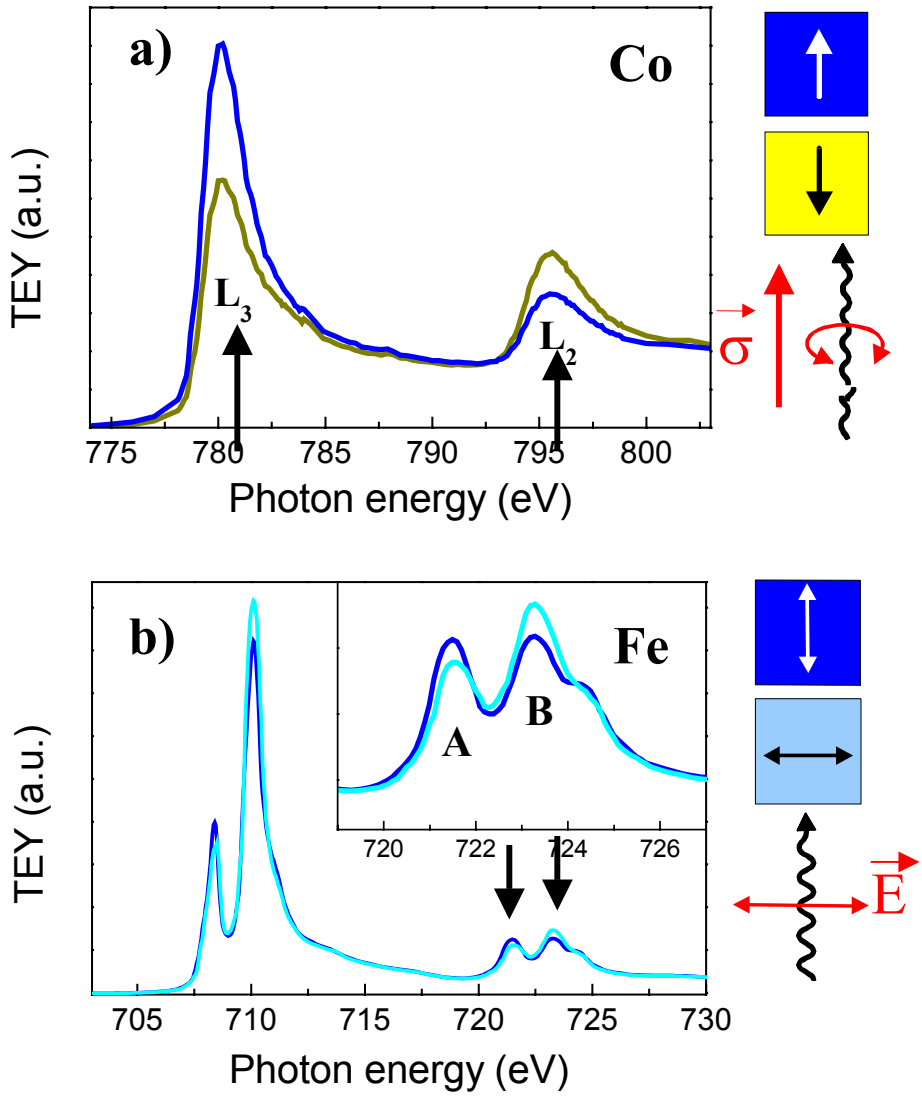
a)
Co
TEY (a.u.)
L3
L2
775
780
785
790
795
800
Photon energy (eV)
σ
b)
Fe
A
B
720
722
724
726
TEY (a.u.)
705
710
715
720
725
730
Photon energy (eV)
E

Figure 4

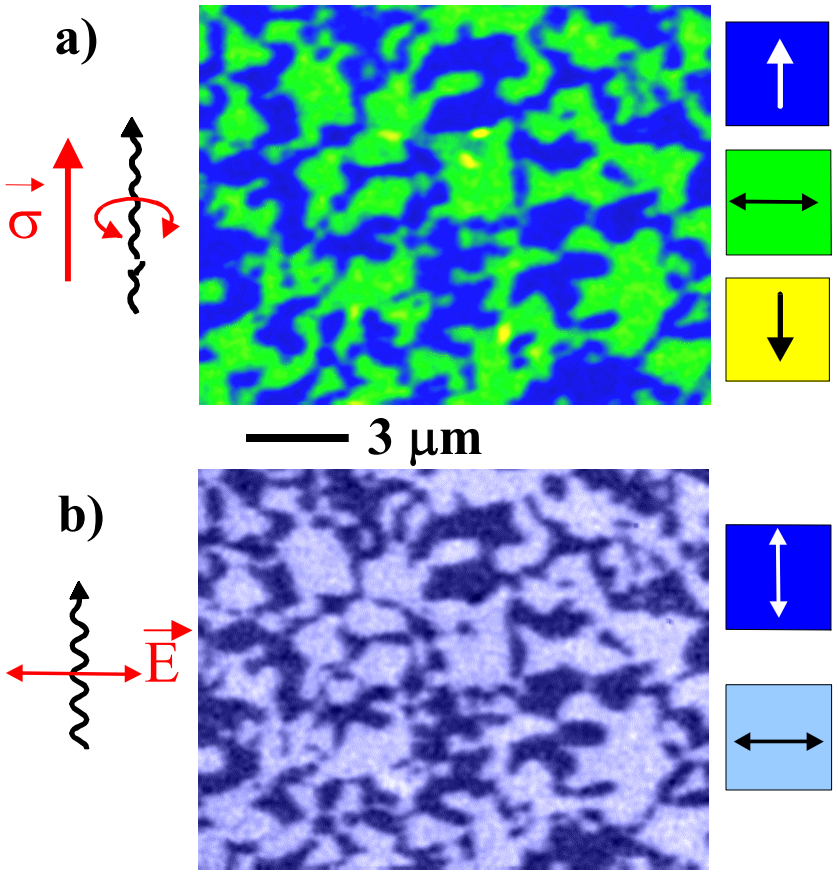

Figure 5

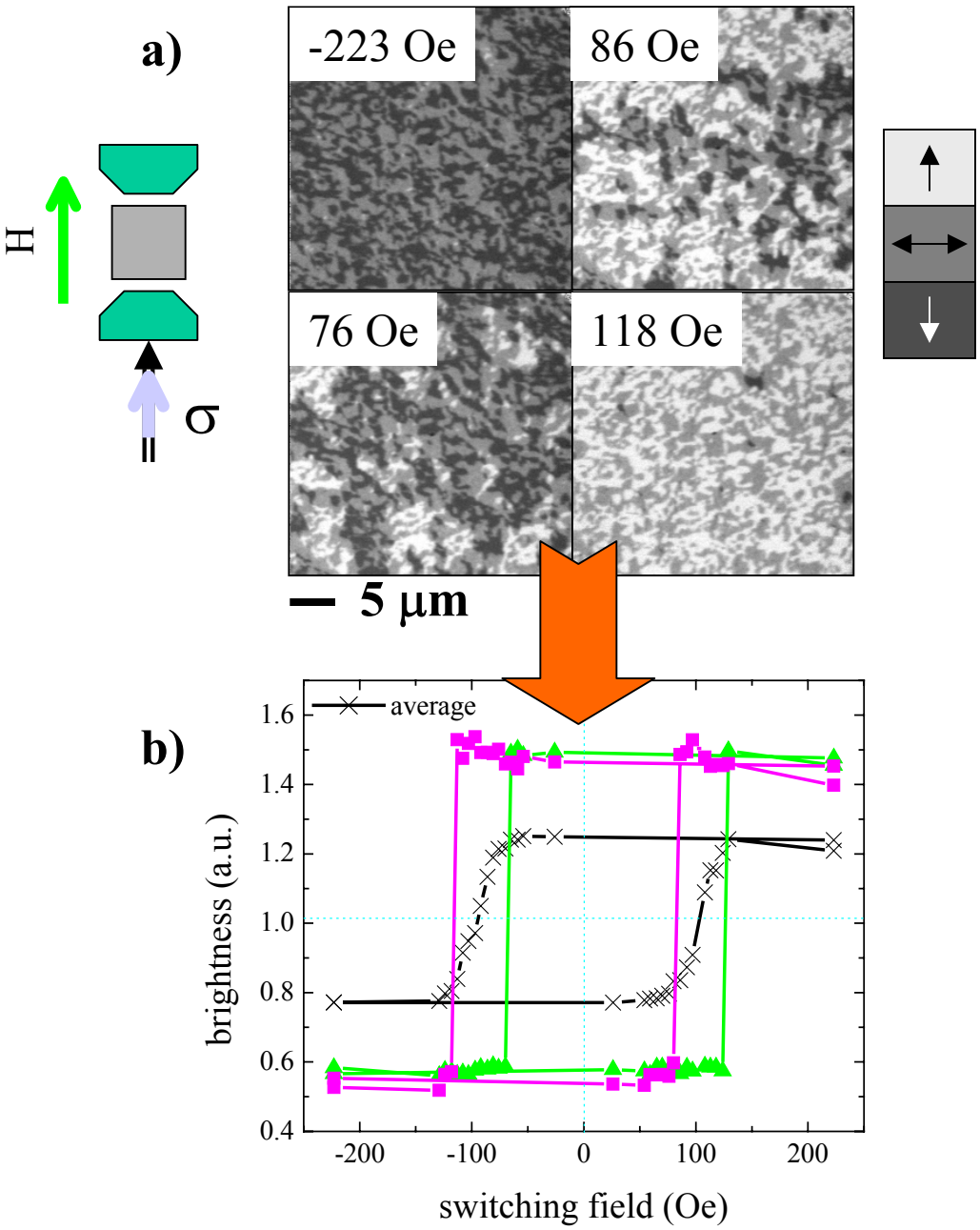
a)
-223 Oe
86 Oe
76 Oe
118 Oe
H
σ
— 5 μm
b)
average
brightness (a.u.)
switching field (Oe)
1.6
1.4
1.2
1.0
0.8
0.6
0.4
-200
-100
0
100
200